Direct Observation of Brownian Motion of Macromolecules by Fluorescence Microscope

INTRODUCTION

The dynamics of flexible polymers in dilute solutions has been studied for a long time by various experimental techniques such as dynamic light scattering, viscoelasticity, dielectric relaxation, and electric birefringence. Although these studies have converged to a successful molecular model (i.e., the Rouse-Zimm model),[1,2] there has been no direct observation of the Brownian motion of flexible polymers. Usually, synthetic polymers are too small to be observed with an optical microscope. However, such natural polymers as DNA can be more than μm, and would be in the visible range for an optical microscope. Indeed, direct observations of DNA have been performed by several workers.[3-5] The technique is to add to a DNA solution a fluorescent dye which is selectively attached to the DNA, and to observe the fluorescence from the dye with a microscope. We used the technique to study the polymer dynamics in dilute solutions, and the results are reported here.

The advantage of the direct observation is the abundance of information; various physical quantities such as the radii of gyration, diffusion constants, and conformational relaxation times can be obtained simultaneously from the video data. This is useful for the direct check of the theory. On the other hand, the method is marred by the fact that the observations have to be done for the solutions sandwiched between two glass plates; the distance between the plates was found to be only a few times larger than the radius of gyration. Thus the walls are expected to affect the polymer dynamics significantly. Indeed we observed that the translational diffusion of DNA is slowed down considerably. On the other hand, the rotational motion around the axis perpendicular to the wall and the monomeric diffusion were found to be close to those described by the Rouse-Zimm model. In particular, we were able to confirm, for the first time, that the mean square displacement of a monomer in a short time t is proportional to $t^{2/3}$.

Keywords: direct observation • fluorescence microscope • DNA • Rouse-Zimm model • dynamic scaling

Journal of Polymer Science: Part B: Polymer Physics, Vol. 30, 779–783 (1992)
 CCC 0887-6266/92/070779-05$04.00

EXPERIMENTAL

The DNA we used is bacteriophage T_4 dC DNA (Nippon Gene), which has 166 kilobase pairs and a contour length of 56 μm. The DNA was diluted with 0.5 × TBE buffer solution (45 mM Tris, 45 mM borate, 1 mM EDTA) containing 4% (v/v) 2-mercaptoethanol, and 4′,6-diamidino-2-phenylindole (DAPI) was added as a fluorescence probe.

The solution was dropped on to a slide glass and covered by a glass plate. The seams of the cover glass were sealed with fingernail polish to prevent thermal convection and evaporation. We made two types of observations with different thicknesses of the liquid layer; the distance between the two plates was 4 μm ("thin samples") and 10 μm ("thick samples").

An inverted microscope (Nikon) with a 100× oil-immersed objective lens and a highly sensitive SIT TV camera with an image processor system (Hamamatsu Photonics) were used with 365 nm ultraviolet (UV) excitation. Two-dimensional real-time image data were recorded on video tapes, and afterwards the data were analyzed with personal computers. Examples of the video data for the thin samples are shown in Figure 1. We were able to get clear images of each molecule continuously for more than several minutes under these conditions. For the thick samples, however, molecules sometimes became defocused during the observation, because the less than 1 μm depth focus makes it very difficult to trace the change of molecular shape, although it may somewhat affect the analysis of the diffusion of the center of mass. Thus we report here the results for rotational relaxation and monomer diffusion using only the thin samples.

The experiments were done for three different DAPI concentrations to check the effects of the probe on the dynamics of DNA in solutions. The concentration of DNA was kept constant at 0.3 μg/ml. The ratio of added DAPI molecules to the number of bases of the DNA was [DAPI]/[DNA] = 0.1, 1.0, and 5.0. The interaction of DAPI and DNA is rather complicated and will be discussed in a separate report.[6]

From the video images, five DNA molecules were selected from each condition, and their conformation data, represented by a set of coordinates $\mathbf{r} \equiv (r_{ix}, r_{iy})$, $(i = 1, \ldots, N)$, were fed to a personal computer with a digitizer every 0.1 second over a period of about 1 minute. To avoid the possble error due to the damage of DNA during manipulation, we chose only the lengthier samples from the

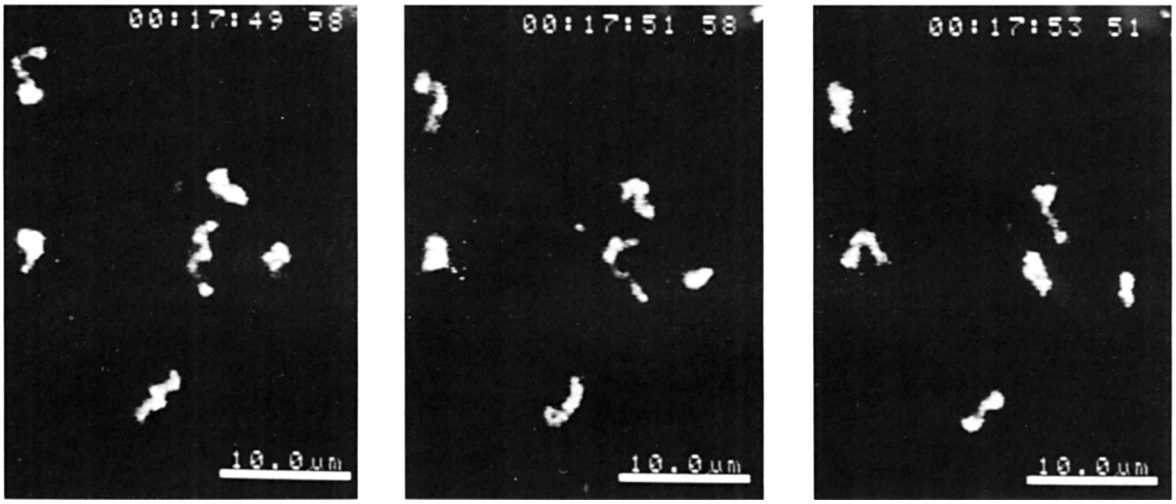

Figure 1. Examples of video image of T_4 DNA molecules in an aqueous solution. Sample thickness is 4 μm and [DAPI]/[DNA] is 1.0. Other experimental conditions are described in the text. The pictures were taken with time interval of 2 s. The scale bar is 10 μm.

video data. We were also careful to discard any samples which appeared to adhere to the glass plates and showed extremely slow mobility. The variation of samples in each condition is shown by error bars in the following figures.

RESULTS AND DISCUSSION

For each conformation, the center of mass

$$R_\alpha(t) = \frac{1}{N}\sum_{i=1}^{N} r_{i\alpha}(t) \qquad (\alpha = x, y) \tag{1}$$

and the radius of gyration tensor

$$T_{\alpha\beta}(t) = \frac{1}{N}\sum_{i=1}^{T} (r_{i\alpha}(t) - R_\alpha(t))(r_{i\beta}(t) - R_\beta(t)) \tag{2}$$

are calculated at each time.

Radius of Gyration

Since we have only two-dimensional information of the segment positions, the radius of gyration R_g is estimated as follows:

$$R_g = (\tfrac{3}{2}(R_l^2 + R_s^2))^{1/2}, \tag{3}$$

where R_l and R_s are the time-average of the larger and smaller principal values of the tensor, respectively. Once R_g is obtained, we can estimate the persistent length λ as follows:[2]

$$\lambda = \frac{3R_g^2}{L}, \tag{4}$$

where L is the contour length of the DNA, 56 μm. The results are shown in Table I. Although the variations among samples are rather large, there is a clear tendency that R_g decreases with increasing DAPI concentration in both samples. A possible cause is that the DAPI bound to DNA reduces the Coulombic repulsion between anionic phosphate groups in the DNA segments. The obtained R_g values of thin samples are larger than those of thick samples, which suggests that the wall effect is not negligible. As seen in Table I, the persistent lengths estimated from thick samples are close to the reported values,[7] 0.0684–0.0820 μm, which were made for Col E1 DNA at low salt concentration with light-scattering technqiue. As far as we know, there have been no reports on the persistent

Table I. Radius of Gyration R_g and Persistent Length λ.

[DAPI]/[DNA]	Thick samples		Thin samples	
	R_g (μm)	λ (μm)	R_g (μm)	λ (μm)
0.1	1.20 ± 0.44	0.077	1.58 ± 0.20	0.134
1.0	1.22 ± 0.42	0.080	1.49 ± 0.21	0.119
5.0	1.08 ± 0.38	0.063	1.33 ± 0.14	0.095

The statistical errors are estimated as the standard deviation of five samples for each condition.

length of T_4 DNA using light-scattering technique, because T_4 DNA is too large.

Translational Diffusion Constant

The translational diffusion constant D_G can be obtained from the mean square displacement of the center of mass in time t. Taking the effect of macroscopic flows into consideration, we used least square fitting to the second order polynomial of t:

$$\langle (\mathbf{R}_G(t) - \mathbf{R}_G(0))^2 \rangle = 4D_G t + At^2, \qquad (5)$$

where $\mathbf{R}_G = (R_x, R_y)$ and A is a numerical constant. Theoretically, D_G is predicted from R_g by the Zimm model as follows:[2]

$$D_G = 0.2030 \frac{k_B T}{\sqrt{6}\eta_s R_g}, \qquad (6)$$

where k_B is the Boltzmann constant and η_s the viscosity of the solvent (1.002 mPas for pure water at $T = 293$ K).

In Figure 2, the calculated values are compared with the experimental results for both the thin and thick samples. The difference between observed and calculated values is large, especially for the thin samples, which suggests that the wall effect is not negligible also for the translational diffusion.

Rotational Relaxation Time

The rotational relaxation time τ_r is obtained from the time correlation function of the unit vector $\mathbf{u}(t)$ parallel to the major principal axis of the tensor $T_{\alpha\beta}$. The correlation function $\langle \mathbf{u}(t) \cdot \mathbf{u}(0) \rangle$ can be well fitted by an exponential curve with single relaxation time τ_r:

$$\langle \mathbf{u}(t) \cdot \mathbf{u}(0) \rangle = \exp(-t/\tau_r). \qquad (7)$$

The theoretical prediction for τ_r is[2]

$$\tau_r = 0.325 \cdot 6^{3/2} \cdot \frac{\eta_s R_g^3}{k_B T}. \qquad (8)$$

In order to obtain continuous clear images of molecules, we used the thin samples for this analysis. The results are

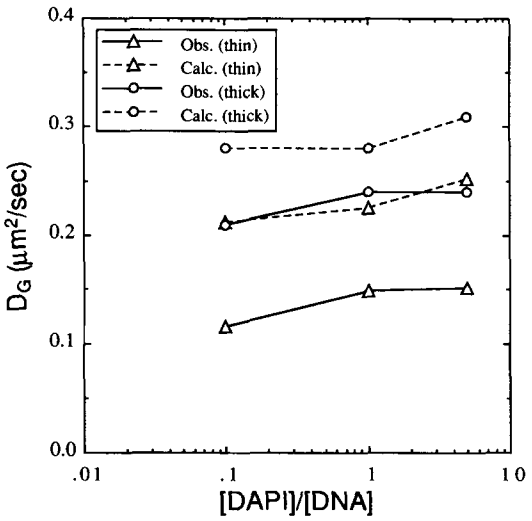

Figure 2. Translational diffusion constant D_G; dashed lines show the values expected from R_g, see eq. (6).

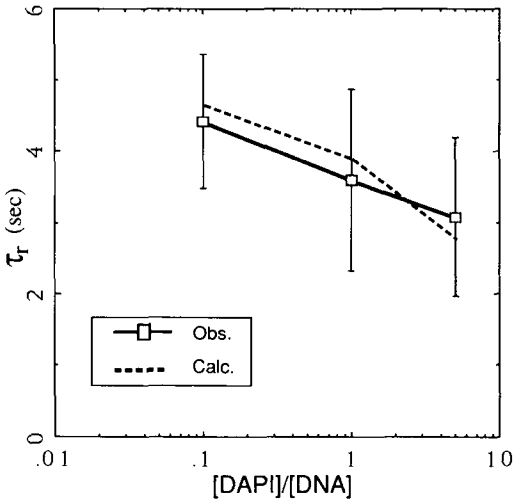

Figure 3. Rotational relaxation time τ_r; the dashed line shows the values expected from R_g, see eq. (8).

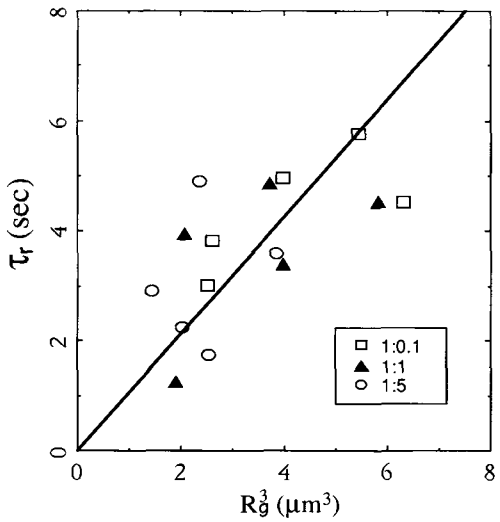

Figure 4. Raw data of R_g and τ_r scattered around the theoretical prediction (solid line), eq. (8).

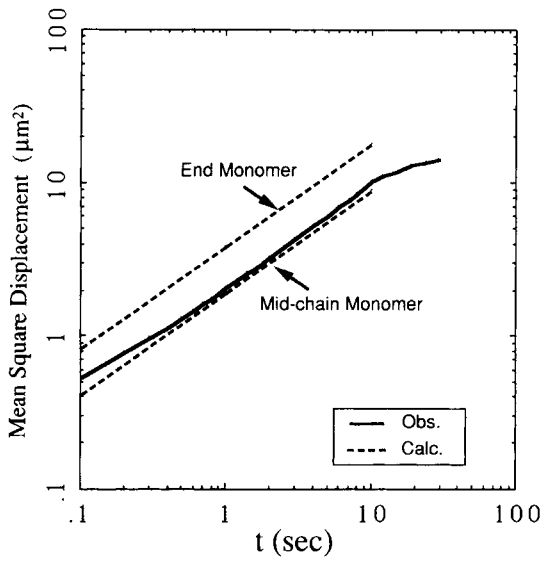

Figure 5. Log-log plot of the mean square displacement of an end monomer in the thin sample with [DAPI]/[DNA] = 10.0. The two dashed lines are the theoretical prediction, see eq. (13).

shown in Figure 3. The agreement between the observation and the prediction is remarkably good. Although the wall affects the rotational motion as it did the translational motion, it appears that the rotational diffusions are less affected by the wall. This is reasonable, since the translational motion is hindered entirely if a part of the chain happens to stick on the wall, but the rotational motion is not. In Figure 3, the scatter in the data points, indicated by the error bars, is large due to the large variation in R_g from sample to sample. However, the obtained relaxation time is found to be close to the theoretical value for each sample. This is seen in Figure 4, where τ_r is plotted against R_g^3 for each sample.

Monomer Diffusion

We also analyzed the mean square displacement $\phi(t)$ of an end monomer,

$$\phi(t) \equiv \langle (\mathbf{r}_N(t) - \mathbf{r}_N(0))^2 \rangle. \tag{9}$$

Since it is essential for this analysis to obtain image data clear enough to identify the end of each molecule, we used the thin samples with [DAPI]/[DNA] = 10.0. The result is shown by a solid line in Figure 5.

The time dependence of $\phi(t)$ can be predicted by a simple scaling law.[1] The system has two basic parameters, R_g as the unit of length and τ_r as the unit of time, so $\phi(t)$ can be written as

$$\phi(t) = R_g^2 f(t/\tau_r), \tag{10}$$

where $f(x)$ is an arbitrary function of x. In the short time region, $\phi(t)$ should be determined only by local properties (temperature, viscosity, etc.) and should be independent of the molecular size. Since τ_r is proportional to R_g^3, this requirement gives

$$\phi(t) \propto R_g^2 \left(\frac{t}{\tau_r}\right)^{2/3} \propto t^{2/3}. \tag{11}$$

The proportionality constant can be calculated by the Rouse-Zimm model. For the two-dimensional observations, the mean square displacement of the n-th segment is given by

$$\phi(t) = 4D_G t + \frac{16N_p\lambda^2}{3\pi^2} \sum_{p=1}^{\infty} \frac{1}{p^2} \times \left(1 + \cos\left(\frac{2\pi n}{N_p}\right)\right)(1 - \exp(-p^{3/2}t/\tau_r)), \tag{12}$$

where $N_p \equiv L/(2\lambda)$ is the number of segments in the polymer. For $t \ll \tau_r$, eq. (12) can be approximated by

$$\phi(t) \simeq \frac{16cN_p\lambda^2}{3\pi^2} \int_0^{\infty} dp p^{-2}(1 - \exp(-p^{3/2}t/\tau_r)) = 0.7645c\left(\frac{k_BT}{\eta_s}\right)^{2/3} t^{2/3}, \tag{13}$$

where $c = 2$ for the very end monomers and 1 for mid-chain monomers. These curves are drawn as dashed lines in Figure 4. Since there is no adjustable parameter in the theoretical curves, it may be said that the agreement is quite good.

In summary, although the wall effects have not been eliminated, our direct observation of the Brownian motion of DNA molecules has confirmed that the Rouse-Zimm model properly describes the polymer dynamics in dilute solutions.

REFERENCES AND NOTES

1. P-G. de Gennes, *Scaling Concepts in Polymer Physics,* Cornell University Press, Ithaca, NY, 1979.
2. M. Doi and S. F. Edwards, *The Theory of Polymer Dynamics,* Clarendon, Oxford, 1986.
3. S. Matsumoto, K. Morikawa, and M. Yanagida, *J. Mol. Biol.,* **152,** 501 (1981).
4. D. C. Schwartz and M. Koval, *Nature,* **338,** 520 (1989).
5. S. B. Smith and A. J. Bendich, *Biopolymers,* **29,** 1167 (1990).
6. K. Minagawa, Y. Matsuzawa, K. Yoshikawa, M. Matsumoto, and M. Doi, in preparation.
7. C. B. Post, *Biopolymers,* **22,** 1087 (1983), and references therein.

MITSUHIRO MATSUMOTO
TOSHIMASA SAKAGUCHI
HIDEYUKI KIMURA
MASAO DOI*

Department of Applied Physics
School of Engineering
Nagoya University
Nagoya 464-01, Japan

KEIJI MINAGAWA
YUKIKO MATSUZAWA
KENICHI YOSHIKAWA

College of General Education
Nagoya University
Nagoya 464-01, Japan

* To whom all correspondence should be addressed.

Received April 29, 1991
Accepted December 3, 1991